AN EXPERIMENTAL STUDY ON THE ADSORPTION OF PER AND POLYFLUOROALKYL SUBSTANCES (PFAS) BY SOIL-DERIVED COLLOIDAL PARTICLES

by

Justin Peschman

A Thesis Submitted in

Partial Fulfillment of the

Requirements for the Degree of

Master of Science

in Geosciences

at

The University of Wisconsin-Milwaukee

August 2024

ABSTRACT

AN EXPERIMENTAL STUDY ON THE ADSORPTION OF PER- AND POLYFLUOROALKYL SUBSTANCES (PFAS) BY SOIL-DERIVED COLLOIDAL PARTICLES

by

Justin Peschman

The University of Wisconsin-Milwaukee, 2024
Under the Supervision of Professor Dr. Shangping Xu

Per- and perfluoroalkyl substances (PFAS) represent a large group of synthesized chemicals that were produced at large scales from the 1930's. As a result of their mass production, large scale commercial use and chemical stability, PFAS have been found ubiquitous within the environment and have been detected in human tissue, bone, and bodily fluids. There are growing concerns about the behavior and mobility of PFAS within the natural environment. Soil represents a major source of PFAS. Although it is well established that soil-derived colloids could facilitate the transport of a wide range of contaminants, there is a significant knowledge gap with regard to the interactions between PFAS and soil colloids. In this research, colloids were collected from intact soil cores that were drilled from agricultural fields located at Pound, WI. A series of experiments were performed to quantify the adsorption of 8 PFAS by the soil-derived colloids. Both synthesized rainwater and local groundwater were used for the adsorption experiments. The results showed that the linear adsorption model could be used to describe the PFAS adsorption behavior and the partitioning coefficient, K_d, were estimated from the

experimental data. These measured PFAS adsorption parameters by soil-derived colloids can be used to develop mathematical models that aim at quantitatively describing PFAS transport within the vadose zone. It was also observed that PFAS adsorption on the soil colloids were stronger in groundwater than in rainwater suggested that colloid-bound PFAS from the vadose zone may continue to move with the colloidal phase rather than become released into the groundwater.

TABLE OF CONTENTS

LIST OF FIGURES

LIST OF TABLES

ACKNOWLEDGEMENTS

I would like to thank my advisor, Dr. Shangping Xu, for his instruction and guidance during not only my thesis, but my entire time at UWM. I admire Shangping's enthusiasm for geoscience and his desire to push the field in new, exciting directions. His expertise and positive attitude have made my experience wholly rewarding, for which I am deeply grateful. I thank Yanan Zhao for her skill in the lab and eagerness to assist with many facets of this project. Without her help this would not have been possible. I thank both Yin Wang and Charlie Paradis for serving on my committee and providing guidance during this challenging process. I would also like to thank my fellow students: Owen Miller, Allison Kusick, and Kamy Veith for their support in the lab.

Additional thanks to Dr. Charlie Paradis who served as my undergraduate research advisor. His support, knowledge and encouragement were vital aspects of my success during both undergraduate and graduate work. I thank everyone in the department for their willingness to help me at a moment's notice. Lastly, I thank my family, especially my wife Allison, for encouraging me and helping me to see this through. Their love and support allowed me to achieve this dream, and I look forward to whatever comes next, because I know they'll be there.

CHAPTER 1: INTRODUCTION

Per- and perfluoroalkyl substances (PFAS) represent a large group of synthesized chemicals that were produced at large scales from the 1930's (Kissa 2001; Paul et al. 2009). Thanks to their numerous desirable properties, PFAS has found use in a wide range of commercial and industrial applications. For instance, their amphiphilic nature and low coefficient of friction makes them ideal for use in things like non-stick cookware, fast food packaging, and water-proof fabrics. The strong carbon-fluorine bonds help to make them non-reactive and desirable for many industrial applications (Buck et al. 2011). These strong chemical bonds also make them resistant to natural degradation allowing them to accumulate in the environment (Eschauzier et al. 2012; Luo and Luo 2007; Merino et al. 2016; Prevedouros et al. 2006). It was estimated that shortly after World War II, perfluorooctanoic acid (PFOA) and perfluorooctane sulfonic acid (PFOS) were put into mass production primarily to be used in the synthesis of polytetrafluoroethylene (PTFE) (Kroll and Nelson 1956; Puts et al. 2019) and many other commercial and industrial products (Buck et al. 2011). The production of PFOS (including its precursors and impurities) ramped up in the 1960's through the 90's peaking at nearly 4500 metric tons per year (Paul et al. 2009). Even after the voluntary discontinuation of PFOA and PFOS production in the United States in 2002 (National Toxicology Program 2016), it is estimated that 6.25 million pounds of 180 different species are still being produced in the United States annually (USEPA 2024).

As a result of their production and commercial use, PFAS have been detected in human tissue, bone, and bodily fluids (Pérez et al. 2013) as well as ice cores in the Arctic (Hartz et al. 2023), and these compounds have become ubiquitous in the environment (Brennan et al. 2021). Over the decades of their production, researchers have discovered the correlations between PFAS and undesirable health effects in animals and humans, though many have only come to light in recent years (Gaber et al. 2023). For instance, recent studies have shown that PFAS can cause high cholesterol, increased liver enzymes, decreased vaccination response, thyroid disorders, pregnancy-induced hypertension and preeclampsia, testicular and kidney cancer, immune suppression, and reduced fertility (USEPA 2023).

The global presence and toxicity of PFAS have been driving the development and enforcement of regulations with the aim to limit human exposures to PFAS. As of April 2024, there is an enforceable limit for six PFAS compounds in drinking water (USEPA 2023). However, ground and surface water standards do not exist nationwide, and some states have enacted their own regulations. For the state of Wisconsin, it is still in the process of making and enforcing these regulations. On the national level, over 6,000 sites are known to be contaminated with many thousands more suspected (EWG 2023). Therefore, as these laws and regulations materialize, it will become essential to understand the full scope of the transport mechanics of PFAS to protect both human and ecological health.

Soil represents a major receiving compartment for PFAS released into the environment. For instance, PFAS are the active ingredients for aqueous film forming foam (AFFF), which has been widely used since the 1970s to fight liquid fuel fires. As a result, soil

contamination has been frequently observed at or near many airports and manufacturing facilities due to past firefighting, training and testing activities (Andrews et al. 2021; Jarvis et al. 2021; Mead & Hunt and LimnoTech 2020; Milley et al. 2018; Persson and Andersson 2016). High concentrations of PFAS can also be introduced into domestic wastewater (Armstrong 2014; Armstrong et al. 2016; Coggan et al. 2019; Johnson 2022; Link et al. 2023; O'Connor et al. 2022; Phong Vo et al. 2020; Robey et al. 2020; Schaider et al. 2016; Thompson et al. 2023; Thompson et al. 2022; Vu and Wu 2022). Thompson et al. (2022) reported the detection of up to 600 ng/L of PFOS, perfluorobutanesulfonic acid (PFBS), perfluorononanoic acid (PFNA), perfluorohexane sulfonate (PFHxS), perfluorobutanoic acid (PFBA), perfluorodecanoic acid (PFDA), perfluoroheptanoic acid (PFHpA), perfluorohexanoic acid (PFHxA) and perfluoropentanoic acid (PFPeA) in the effluents of domestic wastewater treatment plants without any known industrial PFAS sources. It was previously found that the concentrations of PFOS and PFOA in biosolids produced in Marinette County (WI) could be as high as 210,000 and 10,000 ng/g, respectively (WDNR and WDHS 2019). The application of PFAS-contaminated biosolid in agricultural fields could introduce significant quantities of PFAS into the soil (Arcadis 2020; Kaeding 2019; Meyer 2020; WDNR and WDHS 2019).

Within the soil, PFAS can travel through the unsaturated zone to reach the underlying groundwater aquifer, which serves as the primary drinking water source to ~50% of global population (Johnson et al. 2022). Depending on the mobility of PFAS within the contaminated soil, the soil could serve as a long-term source of PFAS to the groundwater system. Very few studies, however, have examined the transport process of PFAS within the

vadose zone (Borthakur et al. 2021; Høisæter et al. 2019; Holly et al. 2024; Lyu et al. 2018; Lyu and Brusseau 2020). Høisæter et al. (2019) reported that the leaching and transport of PFAS within the unsaturated soil led to groundwater contamination of PFAS with an average concentration of 22,000 ng/L (6500-44,000 ng/L). Investigations on PFAS transport within the vadose zone showed that air-water interface could play critical roles in the distribution and mobility of PFAS (Brusseau 2019; Brusseau et al. 2019; Brusseau 2021; Brusseau and Van Glubt 2021; Brusseau and Guo 2022; Costanza et al. 2019; Le et al. 2022; Schaefer et al. 2019; Schaefer et al. 2022; Silva et al. 2021; Wang and Niven 2021). Lyu et al. (2018) and Lyu et al. (2020) investigated the transport of PFOA within unsaturated sediment under steady-state flow conditions and observed that the air-water interface that is unique to unsaturated soil represents major adsorption sites for PFOA, and about 50-75% of total PFOA retention could be attributed to the presence of air-water interface.

The movement of water within the vadose zone is described by the Richards equation which has the following form (Nimmo 2009):

$$q = K(\theta)\left[-\frac{\partial h}{\partial z}\right] = K(\theta)\left[-\frac{\partial(z+\psi)}{\partial z}\right] \quad (1)$$

where q is specific discharge, $K(\theta)$ is the unsaturated hydraulic conductivity which is a function of moisture content θ and associated with soil water retention, h is hydraulic head, which consists of z (elevation head) and ψ (matrix potential head). Factors such as evapotranspiration, precipitation, irrigation and drainage can drive the predominantly vertical movement of water within the unsaturated soil, a process that can subsequently mobilize both dissovled chemicals and particulate matter.

Colloid-sized particles such as clays represent a significant fraction of natural soil. The infiltration of water, and particularly the occurrence of transient conditions (e.g., chemical disturbance, wetting/drying front), within the soil can release large quantities of colloid sized particles and mobilize them toward the underlying groundwater system (Cheng and Saiers 2009; Jin et al. 2023; Levin et al. 2006; Saiers and Hornberger 1996a, b, 1999; Saiers and Lenhart 2003). The mobilized colloid sized particles can in turn facilitate the transport of associated contaminants such as heavy metals, organic compounds and radioactive materials (Saiers and Hornberger 1996a, b; Saiers 2002; Yang et al. 2012).

To my knowledge, very few studies have examined the interactions between soil-derived colloids and PFAS, as well as the roles that the colloids may play in the transport of PFAS within the unsaturated soil. The primary goal of this research is to quantify the adsorption behavior of a group of representative PFAS by colloids released from intact soil cores that were collected from agricultural fields where biosolids from wastewater treatment plants have been applied. The soil-derived colloids were characterized using scanning electron microscopy (SEM) and the adsorption behavior of PFAS by the soil-derived colloids were fitted to relevant adsorption models. The implications of the research findings were then discussed.

CHAPTER 2 MATERIALS AND METHODS

2.1 Soil Cores

The soil cores used for this research were collected from agricultural fields that are located in Pound, WI, with the help of a Geoprobe system using MC7/DT45 liners (diameter: 3 inches). The liners were previously shown to be PFAS free (Rodowa et al. 2020).. The farms have small cattle operations, and grow crops such as corn, soybean and alfalfa. The farms have used biosolids from the nearby wastewater treatment plant in Marinette, WI. Testing of the biosolids have confirmed elevated levels of PFAS that were connected to the nearby Tyco facility which tested AFFF until 2017 (Shute, 2017). However, only very low levels of PFAS were detected at this site.

2.2 Colloid Collection

Colloids were collected for the batch experiments from the soil cores. Briefly, the soil cores were vertically attached to a lab stand and 200 mesh stainless steel membranes were used to cover the bottom of the cores. The stainless-steel membranes were secured to the soil cores with worm gear hose clamps. Polypropylene (PP) funnels were then placed under the core to direct effluent water toward the underlying PP water container.

To mobilize colloids from the soil cores, 50ml of synthetic rainwater was evenly spread onto the top of the cores. This imbibition process was repeated multiple times to accumulate enough material for the subsequent adsorption experiments.

2.3. Colloid Characterization Using SEM

The colloids collected from the soil cores were characterized using Hitachi S-4800 cold cathode field emission SEM and energy-dispersive X-ray spectroscopy (EDS) imaging.

To image the colloids with SEM, the colloid samples were rinsed with HPLC grade water (Fisher Scientific) multiple times and then dried. The rinsing steps were carried out in order to reduce any minerals that could have precipitated during the drying process, which would interfere with imaging and elemental detection. The dried colloids were placed onto a silicon wafer mounted on a 13mm aluminum stub with conductive carbon glue. The samples were then carbon coated in a vacuum coater (Edwards 306A Coating System). The SEM was set to 15kV accelerating voltage in high probe current mode at a 15mm working distance. Images were acquired at 2,000 x magnification. The EDS system was set to auto-detect and allowed to scan for 5 minutes to accumulate elemental makeup information.

2.4 PFAS Adsorption Isotherms

Eight representative PFAS which belong to the perfluorocarboxylic acid (PFCA), perfluorosulfonic acid (PFSA), perfluoroalkyl ether carboxylic acid (PFECA) and fluorotelomer sulfonic acid (FTSA) were selected for this research (**Table 1**). The chemical formula and chemical/physical properties are listed in **Table 1**.

Group	PFCA			PFSA			PFECA	FTSA
Acronym	PFHpA	PFOA	PFNA	PFBS	PFHxS	PFOS	GenX	6:2 FTSA
Molar Mass	364.1	414.1	464.1	300.1	400.1	500.1	347.1	6:2 FTSA
Formula	$C_6F_{13}COOH$	$C_7F_{15}COOH$	$C_8F_{17}COOH$	$C_4F_9SO_3H$	$C_6F_{13}SO_3H$	$C_8F_{17}SO_3H$	$C_3F_7O(CF_2)_2CONH_3$	$C_6F_{13}(CH_2)_2SO_3H$
Density (g/cm^3)	1.792	1.792	1.8	1.824	1.824	1.84-1.85	1.12	428.2
Solubility (mg/L)	44000	9500	12	6875	243	680	740000	1.64-1.71
Vapor Pressure (Pa)	10.0-1998	4.2-1333	1.3-1120	132	48	0.014-17	2910	1323
Log K_{OW}	4.67	5.3	5.92	3.9	5.17	6.3	3.6	0.11
Log K_{OC}	1.52-2.82	1.85-3.77	2.39-2.5	-2.9	2.4	2.6 - 3-5	1.32-1.66	4.44
pK_a	-1.75	0.5-3.8	-1.9	<0.3	<0.3	<0.3-1.2	3.82	2.2-4.9

Table 1.The chemical formula, chemical and physical properties of the 8 representative PFAS used in the batch adsorption experiments.

Precipitation usually represents the main driving force for water infiltration within the unsaturated soil. Additionally, irrigation using groundwater is also a common agricultural practice (Buchwald 2009; Ellefson et al. 2002). For these two scenarios, there can be dramatic difference in water chemistry, which may in turn strong influence the adsorption behavior of PFAS(Lei et al. 2023). In this research, both synthesized rainwater and local groundwater were used for the PFAS adsorption experiments. The major ion concentrations of the synthesized rainwater was based on the average rainwater chemistry measured by National Atmospheric Deposition Program (NADP, https://nadp.slh.wisc.edu/), and the groundwater was collected from a local well. Preliminary testing results showed that all PFAS concentrations in the local groundwater was below detection limit.

If water infiltration is driven by precipitation events, the colloids (and associated PFAS) that leach out of unsaturated soil and enter the underlying groundwater system will experience remarkable water chemistry change. The comparison of PFAS adsorption by soil-derived colloids under two different water chemistry conditions will facilitate the assessment of the fate of PFAS adsorbed on the colloids. For instance, if there is less adsorption of PFAS by the colloids under groundwater conditions, the colloid-bound PFAS can be released as they pass through the water table.

The adsorption experiments were started by mixing the soil-derived colloids and prepared PFAS solutions that contained 100, 500, 1,000, 2,000, 5,000, and 10,000 ng/L of PFAS (as a mixture of all 8 selected PFAS), respectively. The solid to liquid ratio was 100 g

colloids : 1 L liquid in PP tubes. The PP tubes were put on end-to-end shakers for 7 days. Triplicate samples were prepared for each condition.

Once the colloid-liquid mixture was equilibrated for 7 days, the aqueous phase was separated through centrifugation. The supernatant was carefully transferred and mixed with equal volume of methanol (Zhao et al. 2023). An aliquot of acetic acid (0.1%) was then added to adjust the pH to 3 – 4 to enhance PFAS measurement sensitivity in accordance with US EPA method 3512 (U.S.EPA 2021). A mixture of the mass-labeled PFAS was added as the internal standard (**Table 2**).

Table 2. Mass spectrometric conditions used for the measurement of PFAS concentrations using UHPLC-UFMS.

Analyte	Precursor ion (m/z)	Product ion (m/z)	Collision energy (V)	Internal standard	MRL (ng/L)
PFBS	299.1000	80.05	36.0	M3PFBS	10
GenX	285.1000	185.2500	17.0	M3GenX	50
PFHpA	363.0000	318.9500	10.0	M4PFHpA	10
6:2FtS	427.1000	407.1000	20.0	M2-6:2FtS	50
PFOA	413.0000	369.0000	11.0	M8PFOA	10
PFHxS	399.0000	79.95	42.0	M3PFHxS	10
PFNA	463.0000	418.9000	10.0	M9PFNA	10
PFOS	498.9000	80	55.0	M8PFOS	10

The concentration of the PFAS were determined using ultra-high-performance liquid chromatography (UHPLC, Shimadzu Nexera X2) coupled with ultra-fast triple quadrupole mass spectrometery (UFMS, Shimadzu LCMS-8060). Briefly, chromatography was

performed using XB-C18 column (Kinetex® 1.7 µm, 100 Å, 100 x 2.1 mm, Phenomenex). The mobile phase consisted of (A) LC/MS grade water with 20-mM ammonium acetate (Fisher Scientific) and (B) acetonitrile (Optima LCMS grade, Fisher Scientific). The injection volume of each sample was 50 µL and the pumping rate of the mobile phase pump was 400 µL/min. The mobile phases gradient conditions are shown in **Table 3**. The column temperature was maintained at 40 ˚C.

Table 3. The UHPLC-UFMS mobile phase gradient conditions for the measurement of PFAS concentrations.

Time (min)	% Mobile phase (A)	% Mobile phase (B)
0	90	10
2	70	30
9	45	55
11	20	80
13	20	80
14	90	10
15	90	10

The MS/MS analysis was performed on the triple quadrupole UFMS with an electrospray ionization (ESI) source operated at negative mode. The operating conditions are as the following: nebulizing gas flow 3 L/min, heating gas flow 13 L/min, interface temperature 300 °C, desolvation temperature 526 °C, heat block temperature 200 °C, and drying gas flow 5 L/min. The software provided by the manufacturer (Shimadzu LabSolutions V6.82) was used for instrument control, acquisition, and mass analysis. Along with the adsorption aqueous samples, blank control, and PFAS standards were used for quality control purposes. The

concentrations of the 8 PFAS were determined using the isotope dilution technique. The quantity of adsorbed PFAS was then calculated using the mass balance equation (2):

$$Q_e = \frac{(C_0 - C_e) \cdot V}{M} \quad (2)$$

where Q_e (ng/kg) is the amount of PFAS adsorbed onto the soil-derived colloids, C_0 (ng/L) and C_e (ng/L) are the initial and equilibrium PFAS concentrations in the aqueous phase, V (L) is the solution volume, and M (kg) is mass of soil-derived colloids.

Following visual examination of the relationship between Qe and Ce, the adsorption isotherms were fitted with the linear and the Freundlich isotherm models (Wang and Guo 2020):

$$Q_e = K_d \cdot C_e \quad (3)$$

$$Q_e = K_F \cdot C_e^{1/n} \quad (4)$$

where K_d (L/kg) is the linear adsorption constant K_F ((ng/kg)·(L/ng)$^{1/n}$) is the Freundlich constant, n is a dimensionless indicator related to the adsorption heterogeneity (Wang and Guo 2020; Zhao et al. 2023).

CHAPTER 3 RESULTS AND DISCUSSION

3.1 Colloid Characterization

The SEM image of the soil-derived colloids is shown in **Figure 1**. The size of most of colloids was ~ 1 μm range, and there were a few larger aggregates (~5-6 μm). In general, the colloidal particles had clear edges and exhibited shapes of cubes. The EDS results showed that in addition to Si, there were significant amounts of Al, Fe, K and Mg, suggesting that the colloids could contain iron (hydr)oxides and clays.

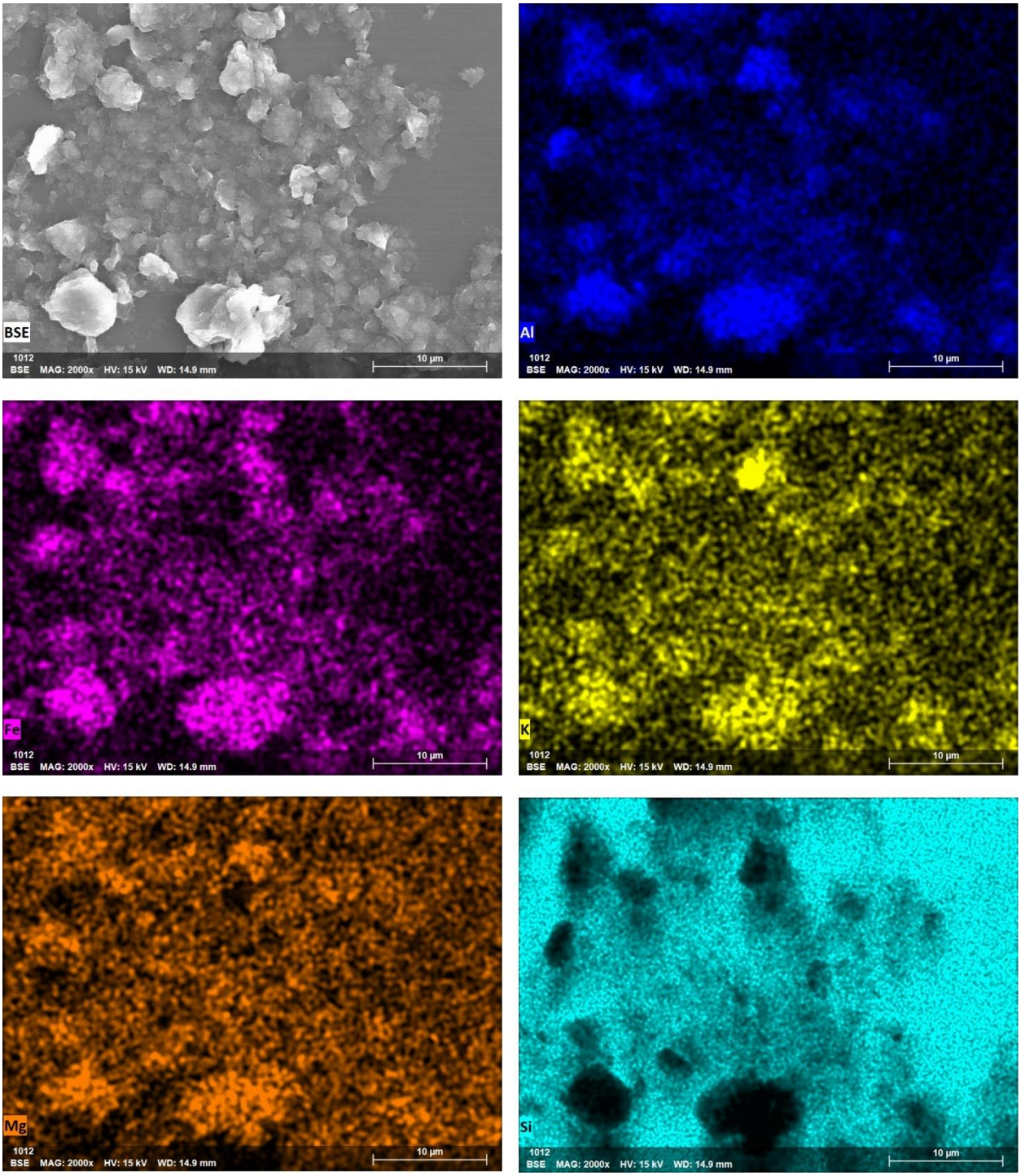

Figure 1. The SEM and EDS (Al, Fe, K, Mg, and Si) images for the soil-derived colloids.

3.2 Adsorption Isotherms

The adsorption isotherms obtained using synthesized rainwater were fitted to both the linear and Freundlich models (**Figures 2 and 3**). The isotherm plots are organized into PFCA, PFSA, FTSA and PFECA groups based on their chemical structures.

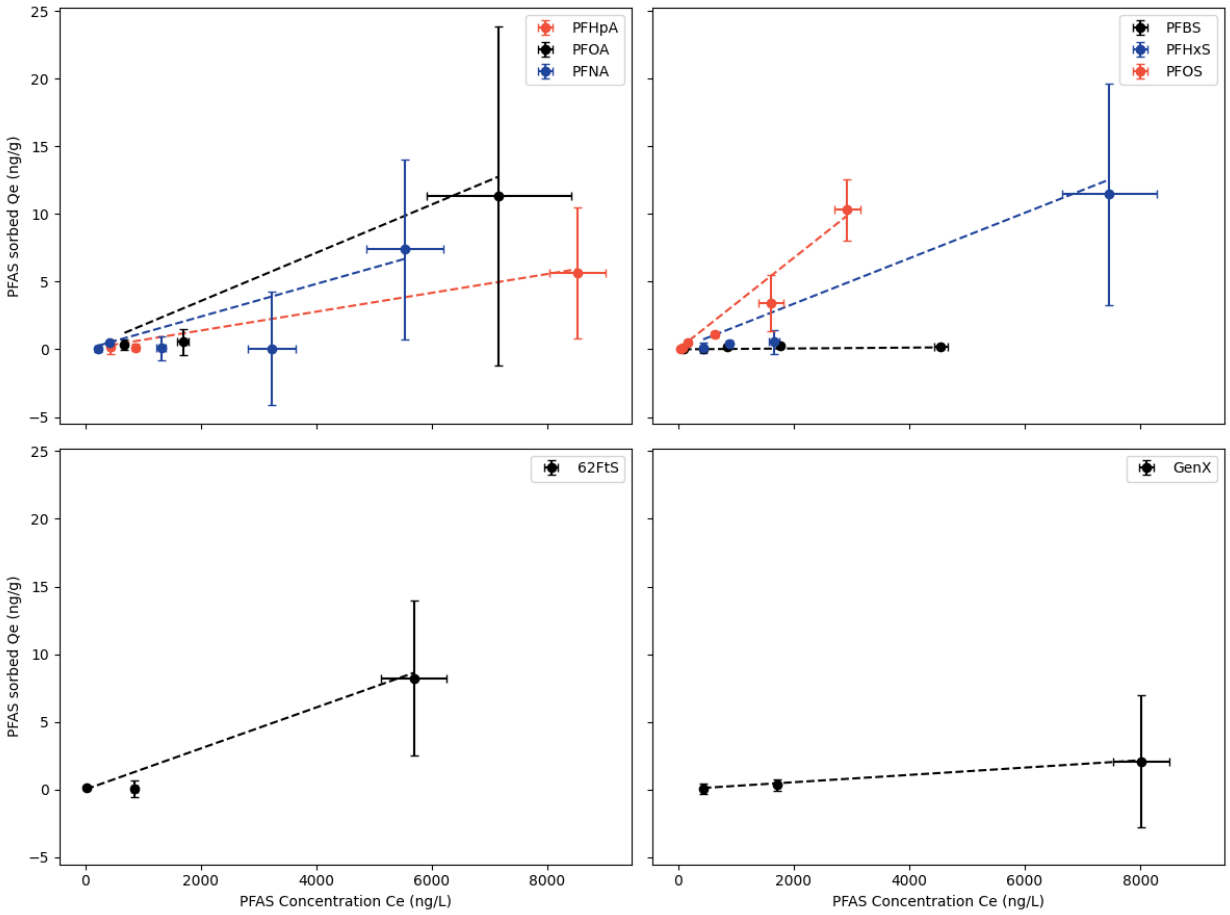

Figure 2. PFAS adsorption isotherms by soil-derived colloids in synthesized rainwater. The lines represent the fitted linear model. The PFAS were organized into PFCA, PFSA, FTSA and PFECA groups.

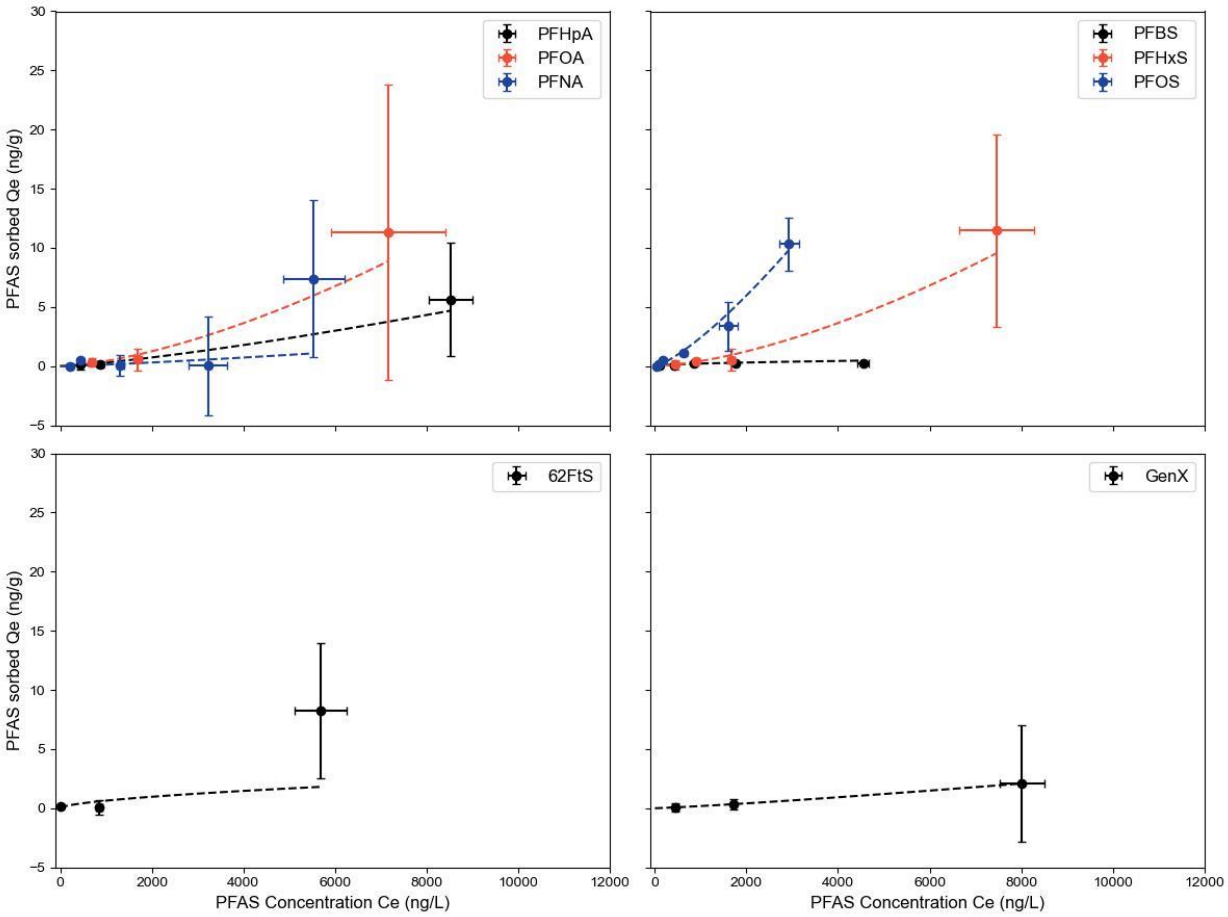

Figure 3. PFAS adsorption isotherms by soil-derived colloids in synthesized rainwater. The lines represent the fitted Freundlich model. The PFAS were organized into PFCA, PFSA, FTSA and PFECA groups.

Similarly, the adsorption isotherms obtained using local groundwater as well as the fitted linear and Freundlich models are shown in **Figures 4 and 5**.

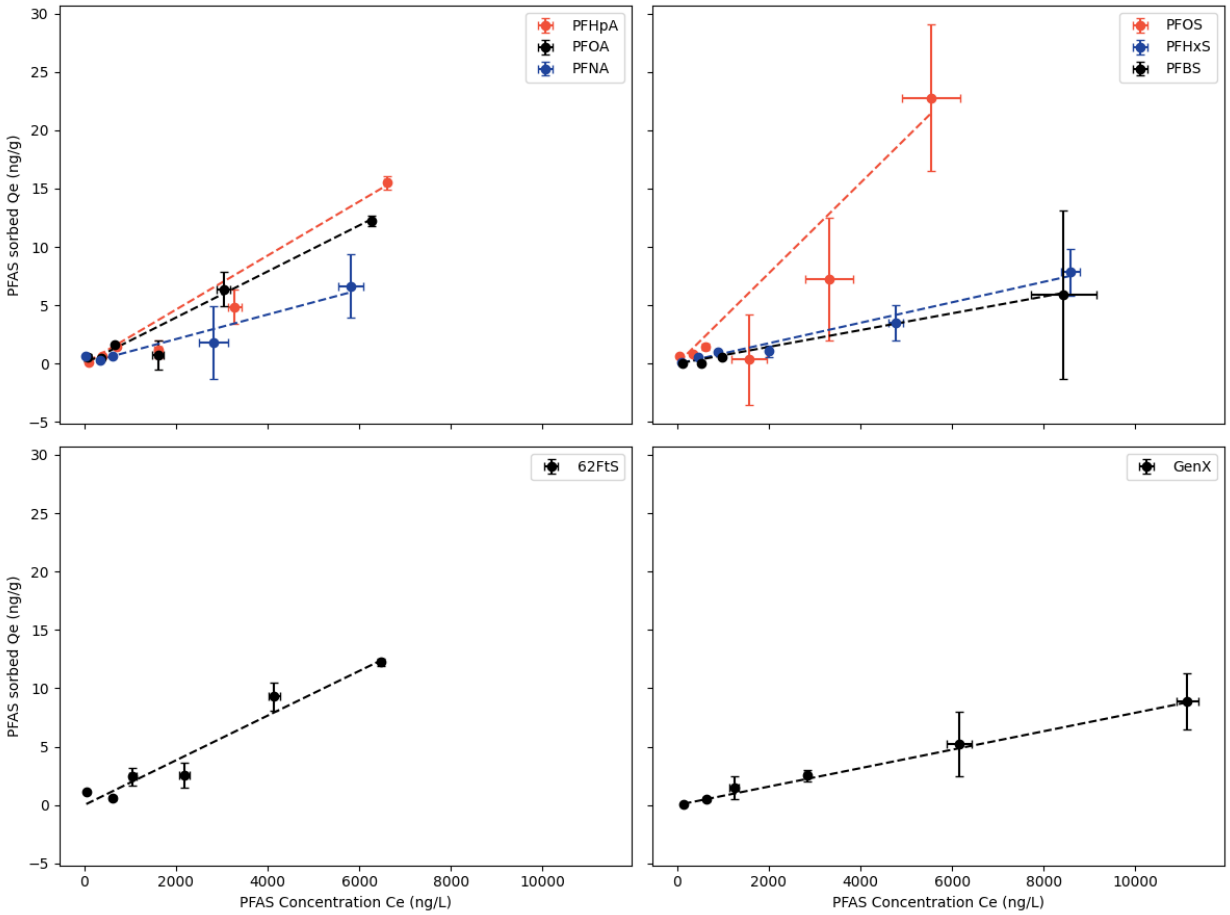

Figure 4. PFAS adsorption isotherms by soil-derived colloids in local groundwater. The lines represent the fitted linear model. The PFAS were organized into PFCA, PFSA, FTSA and PFECA groups.

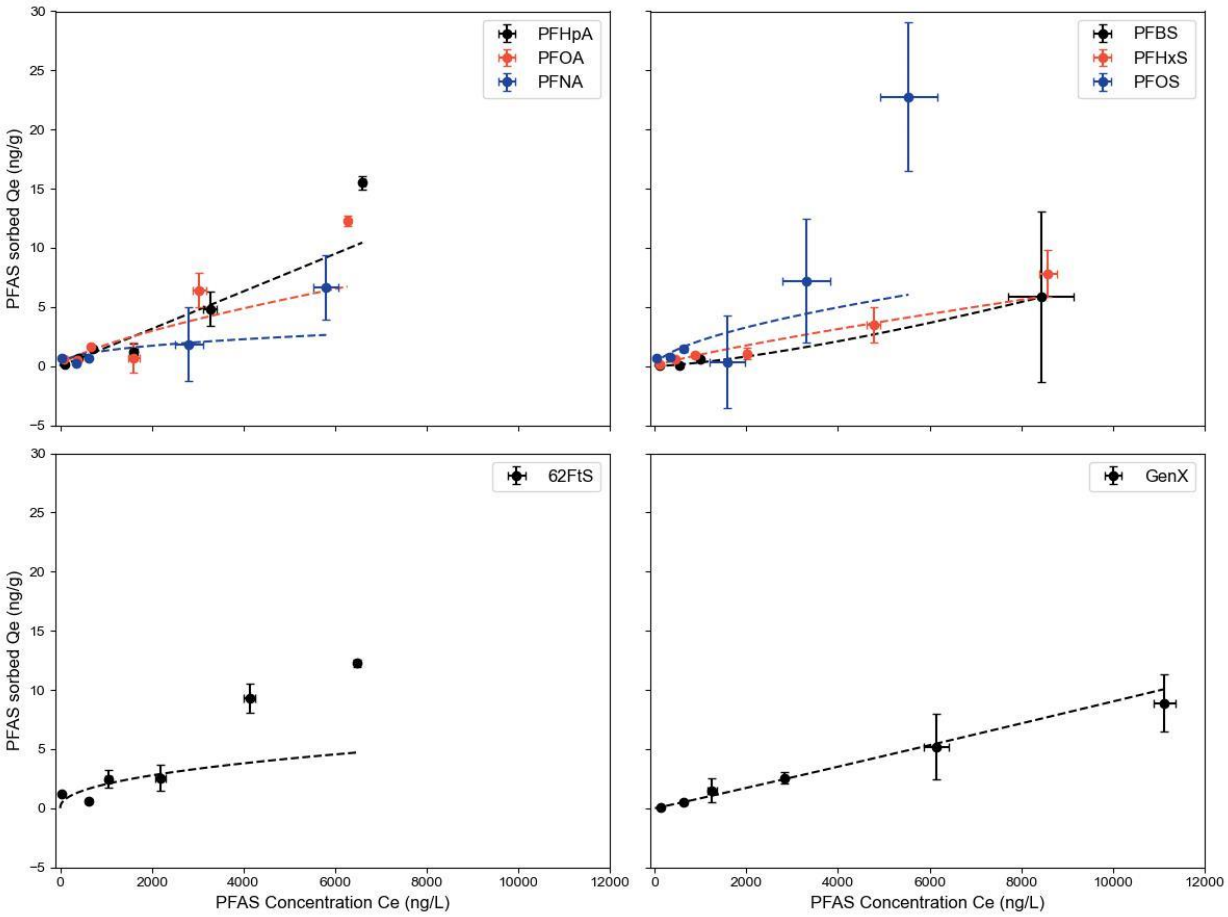

Figure 5. PFAS adsorption isotherms by soil-derived colloids in local groundwater. The lines represent the fitted Freundlich model. The PFAS were organized into PFCA, PFSA, FTSA and PFECA groups.

As can be seen from the comparison of the experimental isotherm data and the fitting models, as well as the R^2 values, both the linear model and Freundlich model can successfully be used to describe the adsorption of the 8 selected PFAS by the soil-derived colloids under the rainwater and groundwater conditions. It seems that although the Freundlich model has one extra degree of freedom in model fitting, it generally did not perform as well as the linear model. For the linear model, the summation of R^2 (ΣR^2) for the rainwater and groundwater cases were 7.768 and 7.662, respectively. In contrast, for the Freundlich model, the summation of R^2 (ΣR^2) for the rainwater and groundwater cases were 7.556 and 7.118. Considering that the values of K_d, which describes the portioning of PFAS between the aqueous phase and the colloidal phase, have been widely used to describe the adsorption behavior of a large number of chemicals by various materials and have been commonly used to quantitatively describe the transport behavior of chemicals within the natural environment, the following discussion will be primarily focused on the values of K_d

The estimated K_d values ranged between 0.257 (L/kg, GenX, rainwater) and 3.402 (L/kg, PFOS, groundwater). Although cautions need to be applied when comparing K_d

values obtained from different studies, the K_d values quantified in this research are consistent to previous reported values (Knight et al. 2019; Kookana et al. 2023; Li et al. 2018; Nguyen et al. 2020; Oliver et al. 2019, 2020). For instance, Zhao et al. (2023) observed that the adsorption of PFAS by 6 different types of sediments ranged from 0.6 (L/kg, PFBS) to 11.284 (L/kg, PFOS). Nguyen et a. (2020) reported that the adsorption of GenX by 10 soils under field pH conditions ranged from 0.007 to 0.40 (L/kg), and the value of 0.257 (L/kg) fell within this range. Noticeably, the K_d values for GenX are generally lower than the other tested PFAS chemicals. This could be related to the fact that GenX has one of the lowest charge density (13.8 meq/g C) (Dixit et al. 2020). Additionally, the ether bond in the GenX molecule could lead to the instability of the negatively charged head, and as a result, the affinity of GenX to adsorbents was often lower than that of PFOA (Kancharla et al. 2022; Wang et al. 2019). On the other end of the spectrum, the measured K_d values of PFOS were between 3.22 and 34.2 (L/kg) (Nguyen et al. 2020), and the estimated K_d value of PFOS from this research compared favorably to the lower range of the reported values.

3.3 Effects of Water Chemistry on PFAS Adsorption

In this research, the adsorption of the 8 selected by the soil-derived colloids were studied using both synthesized rainwater and local groundwater, which had remarkably different water chemistry. For the rainwater, the total dissolved solid (TDS) was ~ 6 mg/L and the pH was ~ 5.2 For the local groundwater, the TDS was ~ 633 mg/L and the pH was ~ 8.1. The results would allow us to assess the roles of soil-derived colloids in PFAS behavior and transport within the vadose zone under two different scenarios: infiltration driven by precipitation, or infiltration caused by irrigation using groundwater.

The comparison of the K_d values under the two different water chemistry conditions showed that there was generally stronger adsorption of the PFAS (except for PFNA and PFHxS) by the soil-derived colloids when they were suspended in groundwater (**Figure 6**). This finding also implied that once the soil-derived colloids were mobilized into the underlying groundwater system, it would be unlikely that the adsorbed PFAS would be released into the aqueous phase. The fate of the colloid-bound PFAS within the groundwater aquifer would thus be determined by the mobility of the colloids.

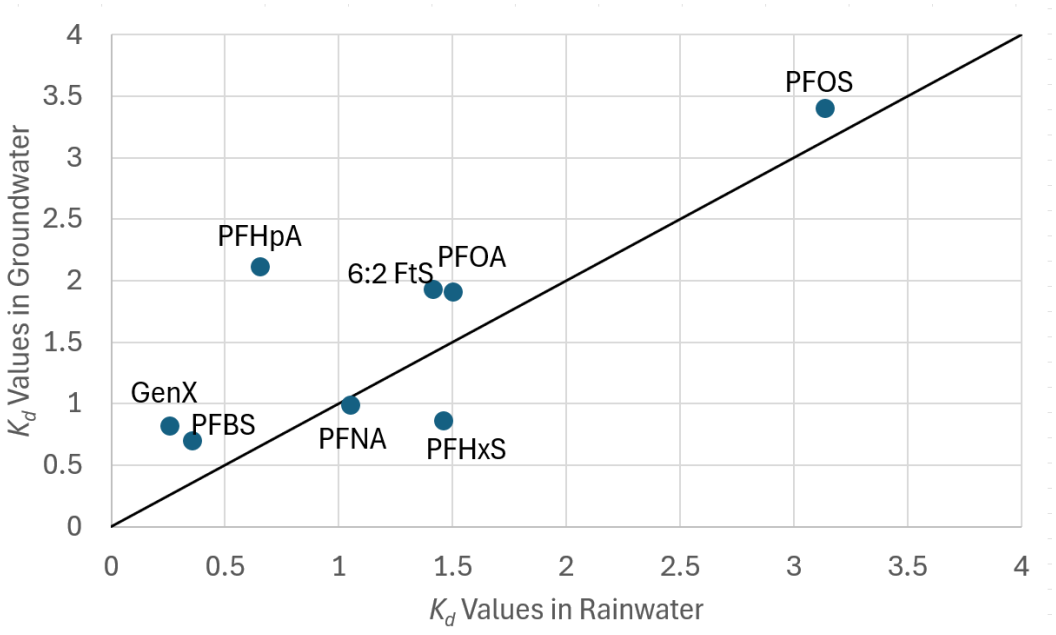

Figure 6. Comparison of the Kd values obtained under rainwater and groundwater conditions for the selected 8 PFAS. For chemicals that are above the 1:1 line, their adsorption by the colloids was stronger in groundwater than in rainwater.

The adsorption of PFAS by soil components, including soil-derived colloids, could be influenced by a larger number of factors, and the underlying mechanisms could include

processes such as electrostatic interactions, hydrophobic interactions, hydrogen bonding, as well as ligand and ion exchange (Feng et al. 2024; Kabiri et al. 2024; Kookana et al. 2023; Li et al. 2019; Liu et al. 2020; Luft et al. 2022; Nguyen et al. 2020; Wanzek et al. 2023; Wei et al. 2017; Zhou et al. 2021). Most of the PFCAs and PFSAs have low *pKa* values (**Table 1**) and they are present in the anionic form under ambient pH conditions (4-9) (Kookana et al. 2023). For GenX, it is also negatively charged but has one of the lowest charge density (13.8 meq/g C) (Dixit et al. 2020) and the negatively charged head could be unstable due to the presence of the ether bond (Kancharla et al. 2022; Wang et al. 2019). For the soil-derived colloids examined in this research, the electrostatic interactions and the ion exchange could be primarily responsible for PFAS adsorption. These two processes could be strongly influenced by the distribution and density of the charges on the surface of iron (hydr)oxides and clay minerals, which in turn could be determined by water chemistry conditions. In general, higher electrolyte solutions could lower charge density within the electrostatic double layer (EDL) and thus could enhance the adsorption of the negatively charged PFAS (Israelachvili 1991). For instance, for similarly negatively charged arsenate, when the pH was above the *pKa*, higher ionic strength enhanced its adsorption by iron (hydr)oxides (Mamindy-Pajany et al. 2009).

3.4 Effects of PFAS Chemical Structure on PFAS Adsorption

The adsorption behavior of PFAS was found to be closely related to the structure and chemical properties of the PFAS (Kookana et al. 2023; Nguyen et al. 2020; Zhao et al. 2023). For instance, Nguyen et al. (2020) reported that the adsorption of a large number of

PFAS by soil was chain length-dependent, and were significantly linearly related to molecular weight.

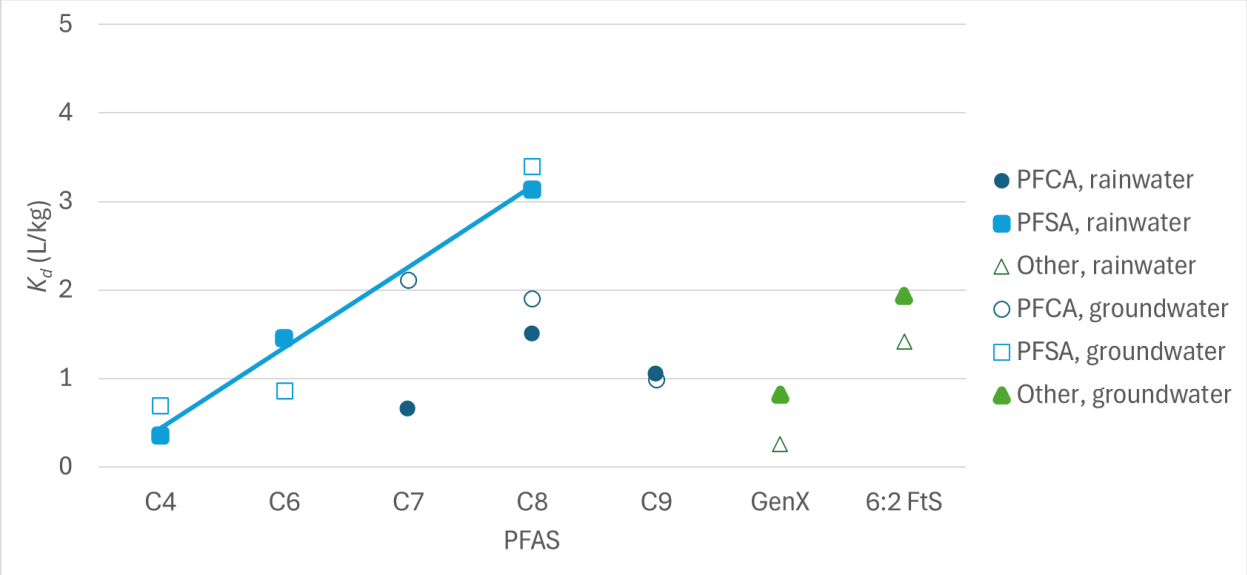

Figure 7. The Kd values for the 8 PFASs as a function of perfluorinated C-chain length for PFCAs, PFSAs, GenX and 6:2 FtS obtained under rainwater and groundwater. The Kd values for the PFSAs linearly increased with C-chain length as indicated by the regression line.

The K_d values measured in this research showed that the K_d values for the PFSAs linearly increased with C-chain length (**Figure 7**). The K_d values for PFCAs, however, were similar and varied less, and there was no discernable trend between the K_d values and the C-chain length.

CHAPTER 4 ENVIRONMENTAL IMPLICATIONS

Our understanding of the behavior and mobility of PFAS within the soil environment is critical to the evaluation of PFAS pollution in both surface water and groundwater systems, to the assessment of associated public health risks, and the design and implementation of remediation strategies. Although it is well established that soil-derived colloids could facilitate the transport of a wide range of contaminants, there is a significant knowledge gap with regard to the interactions between PFAS and soil colloids. The measured PFAS adsorption parameters by soil-derived colloids can be used to develop mathematical models that aim at quantitatively describing PFAS transport within the vadose zone. The observation that PFAS adsorption on the soil colloids were stronger in groundwater than in rainwater suggested that colloid-bound PFAS from the vadose zone may continue to move with the colloidal phase rather than become released into the groundwater.

REFERENCES

Andrews DQ, Hayes J, Stoiber T, Brewer B, Campbell C, Naidenko OV. 2021. Identification of point source dischargers of per- and polyfluoroalkyl substances in the united states. AWWA Water Science 3:e1252.

Arcadis. 2020. Drinking water well sampling summary report - land applied biosolids area, marinette and oconto counties, wisconsin.

Armstrong DL. 2014. Temporal trends and influence of storage methods on concentrations of perfluoroalkyl substances in limed municipal wastewater biosolids [M.S.]. Ann Arbor:University of Maryland, College Park.

Armstrong DL, Lozano N, Rice CP, Ramirez M, Torrents A. 2016. Temporal trends of perfluoroalkyl substances in limed biosolids from a large municipal water resource recovery facility. Journal of Environmental Management 165:88-95.

Borthakur A, Cranmer BK, Dooley GP, Blotevogel J, Mahendra S, Mohanty SK. 2021. Release of soil colloids during flow interruption increases the pore-water pfas concentration in saturated soil. Environmental Pollution 286:117297.

Brennan NM, Evans AT, Fritz MK, Peak SA, von Holst HE. 2021. Trends in the regulation of per- and polyfluoroalkyl substances (pfas): A scoping review. Int J Environ Res Public Health 18.

Brusseau ML. 2019. Estimating the relative magnitudes of adsorption to solid-water and air/oil-water interfaces for per- and poly-fluoroalkyl substances. Environmental Pollution 254:113102.

Brusseau ML, Yan N, Van Glubt S, Wang Y, Chen W, Lyu Y, et al. 2019. Comprehensive retention model for pfas transport in subsurface systems. Water Research 148:41-50.

Brusseau ML. 2021. Examining the robustness and concentration dependency of pfas air-water and napl-water interfacial adsorption coefficients. Water Research 190:116778.

Brusseau ML, Van Glubt S. 2021. The influence of molecular structure on pfas adsorption at air-water interfaces in electrolyte solutions. Chemosphere 281:130829.

Brusseau ML, Guo B. 2022. Pfas concentrations in soil versus soil porewater: Mass distributions and the impact of adsorption at air-water interfaces. Chemosphere 302:134938.

Buchwald CA. 2009. Water use in wisconsin, 2005. (USGS Open-File Report 2009–1076).

Buck RC, Franklin J, Berger U, Conder JM, Cousins IT, de Voogt P, et al. 2011. Perfluoroalkyl and polyfluoroalkyl substances in the environment: Terminology, classification, and origins. Integr Environ Assess Manag 7:513-541.

Cheng T, Saiers JE. 2009. Mobilization and transport of in situ colloids during drainage and imbibition of partially saturated sediments. Water Resources Research 45:W08414, doi:08410.01029/02008WR007494.

Coggan TL, Moodie D, Kolobaric A, Szabo D, Shimeta J, Crosbie ND, et al. 2019. An investigation into per- and polyfluoroalkyl substances (pfas) in nineteen australian wastewater treatment plants (wwtps). Heliyon 5.

Costanza J, Arshadi M, Abriola LM, Pennell KD. 2019. Accumulation of pfoa and pfos at the air–water interface. Environmental Science & Technology Letters 6:487-491.

Dixit F, Barbeau B, Mostafavi SG, Mohseni M. 2020. Efficient removal of genx (hfpo-da) and other perfluorinated ether acids from drinking and recycled waters using anion exchange resins. Journal of Hazardous Materials 384:121261.

Ellefson BR, Mueller GD, Buchwald CA. 2002. Water use in wisconsin, 2000. U. S. Geological survey open-file report 02–356.

Eschauzier C, Beerendonk E, Scholte-Veenendaal P, De Voogt P. 2012. Impact of treatment processes on the removal of perfluoroalkyl acids from the drinking water production chain. Environmental science & technology 46:1708-1715.

EWG. 2023. Mapping the pfas contamination crisis: New data show 4,621 sites in 50 states, the district of columbia and two territories.

Feng G, Zhou B, Yuan R, Luo S, Gai N, Chen H. 2024. Influence of soil composition and environmental factors on the adsorption of per- and polyfluoroalkyl substances: A review. Science of The Total Environment 925:171785.

Gaber N, Bero L, Woodruff TJ. 2023. The devil they knew: Chemical documents analysis of industry influence on pfas science. Annals of Global Health.

Hartz WF, Björnsdotter MK, Yeung LWY, Hodson A, Thomas ER, Humby JD, et al. 2023. Levels and distribution profiles of per- and polyfluoroalkyl substances (pfas) in a high arctic svalbard ice core. Science of The Total Environment 871:161830.

Høisæter Å, Pfaff A, Breedveld GD. 2019. Leaching and transport of pfas from aqueous film-forming foam (afff) in the unsaturated soil at a firefighting training facility under cold climatic conditions. Journal of Contaminant Hydrology 222:112-122.

Holly MA, Gunn KM, Keymer D, Sanford JR. 2024. Evaluation of per- and polyfluoroalkyl substances leaching from biosolids and mitigation potential of biochar through undisturbed soil columns. ACS ES&T Water 4:413-426.

Israelachvili JN. 1991. Intermolecular and surface forces. 2nd ed. London ; San Diego:Academic Press.

Jarvis AL, Justice JR, Elias MC, Schnitker B, Gallagher K. 2021. Perfluorooctane sulfonate in us ambient surface waters: A review of occurrence in aquatic environments and comparison to global concentrations. Environmental Toxicology and Chemistry 40:2425-2442.

Jin Y, Shen C, Lazouskaya V. 2023. Colloid transport. In: Encyclopedia of soils in the environment (second edition), (Goss MJ, Oliver M, eds). Oxford:Academic Press, 336-352.

Johnson GR. 2022. Pfas in soil and groundwater following historical land application of biosolids. Water Research 211:118035.

Johnson TD, Belitz K, Kauffman LJ, Watson E, Wilson JT. 2022. Populations using public-supply groundwater in the conterminous u.S. 2010; identifying the wells, hydrogeologic regions, and hydrogeologic mapping units. Science of The Total Environment 806:150618.

Kabiri S, Monaghan CL, Navarro D, McLaughlin MJ. 2024. Hydrophobic interaction is the dominant mechanism of zwitterionic pfas adsorption to carbon-based sorptive materials in water and soil. Environmental Science: Water Research & Technology 10:420-430.

Kaeding D. 2019. Residents concerned about pfas contamination on farm fields in marinette, peshtigo area.

Kancharla S, Choudhary A, Davis RT, Dong D, Bedrov D, Tsianou M, et al. 2022. Genx in water: Interactions and self-assembly. Journal of Hazardous Materials 428:128137.

Kissa E. 2001. Fluorinated surfactants and repellents:CRC Press.

Knight ER, Janik LJ, Navarro DA, Kookana RS, McLaughlin MJ. 2019. Predicting partitioning of radiolabelled 14c-pfoa in a range of soils using diffuse reflectance infrared spectroscopy. Science of The Total Environment 686:505-513.

Kookana RS, Navarro DA, Kabiri S, McLaughlin MJ. 2023. Key properties governing sorption–desorption behaviour of poly- and perfluoroalkyl substances in saturated and unsaturated soils: A review. Soil Res 61:107-125.

Kroll AE, Nelson DA. 1956. Polymerization of tetrafluoroethylene with tertiary butyl peroxide or peracetate. (Office USPaT, ed). United States.

Le S-T, Gao Y, Kibbey TCG, Glamore WC, O'Carroll DM. 2022. Predicting the impact of salt mixtures on the air-water interfacial behavior of pfas. Science of The Total Environment 819:151987.

Lei X, Lian Q, Zhang X, Karsili TK, Holmes W, Chen Y, et al. 2023. A review of pfas adsorption from aqueous solutions: Current approaches, engineering applications, challenges, and opportunities. Environmental Pollution 321:121138.

Levin JM, Herman JS, Hornberger GM, Saiers JE. 2006. Colloid mobilization from a variably saturated, intact soil core. Vadose Zone Journal 5:564-569.

Li F, Fang X, Zhou Z, Liao X, Zou J, Yuan B, et al. 2019. Adsorption of perfluorinated acids onto soils: Kinetics, isotherms, and influences of soil properties. Science of The Total Environment 649:504-514.

Li Y, Oliver DP, Kookana RS. 2018. A critical analysis of published data to discern the role of soil and sediment properties in determining sorption of per and polyfluoroalkyl substances (pfass). Science of The Total Environment 628-629:110-120.

Link GW, Reeves DM, Cassidy DP, Coffin ES. 2023. Per- and polyfluoroalkyl substances (pfas) in final treated solids (biosolids) from 190 michigan wastewater treatment plants. Journal of Hazardous Materials:132734.

Liu Y, Qi F, Fang C, Naidu R, Duan L, Dharmarajan R, et al. 2020. The effects of soil properties and co-contaminants on sorption of perfluorooctane sulfonate (pfos) in contrasting soils. Environ Technol Inno 19:100965.

Luft CM, Schutt TC, Shukla MK. 2022. Properties and mechanisms for pfas adsorption to aqueous clay and humic soil components. Environmental Science & Technology 56:10053-10061.

Luo Y-R, Luo Y-R. 2007. Comprehensive handbook of chemical bond energies. Boca Raton:CRC Press.

Lyu Y, Brusseau ML, Chen W, Yan N, Fu X, Lin X. 2018. Adsorption of pfoa at the air–water interface during transport in unsaturated porous media. Environmental Science & Technology 52:7745-7753.

Lyu Y, Brusseau ML. 2020. The influence of solution chemistry on air-water interfacial adsorption and transport of pfoa in unsaturated porous media. Science of The Total Environment 713:136744.

Mamindy-Pajany Y, Hurel C, Marmier N, Roméo M. 2009. Arsenic adsorption onto hematite and goethite. Comptes Rendus Chimie 12:876-881.

Mead & Hunt I, LimnoTech. 2020. Former firefighting training areas soil and groundwater sampling summary dane county regional airport.

Merino N, Qu Y, Deeb RA, Hawley EL, Hoffmann MR, Mahendra S. 2016. Degradation and removal methods for perfluoroalkyl and polyfluoroalkyl substances in water. Environmental Engineering Science 33:615-649.

Meyer B. 2020. Rhinelander spread tons of sludge near site of contaminated wells, wxpr investigation finds.

Milley SA, Koch I, Fortin P, Archer J, Reynolds D, Weber KP. 2018. Estimating the number of airports potentially contaminated with perfluoroalkyl and polyfluoroalkyl substances from aqueous film forming foam: A canadian example. Journal of Environmental Management 222:122-131.

National Toxicology Program. 2016. Immunotoxicity associated with exposure to perfluorooctanoic acid (pfoa) or perfluorooctane sulfonate (pfos). 335-67-1; 1763-23-1.

Nguyen TMH, Bräunig J, Thompson K, Thompson J, Kabiri S, Navarro DA, et al. 2020. Influences of chemical properties, soil properties, and solution ph on soil–water partitioning coefficients of per- and polyfluoroalkyl substances (pfass). Environmental Science & Technology 54:15883-15892.

Nimmo JR. 2009. Vadose water. In: Encyclopedia of inland waters, (Likens GE, ed). Oxford:Academic Press, 766-777.

O'Connor J, Bolan NS, Kumar M, Nitai AS, Ahmed MB, Bolan SS, et al. 2022. Distribution, transformation and remediation of poly- and per-fluoroalkyl substances (pfas) in wastewater sources. Process Saf Environ 164:91-108.

Oliver DP, Li Y, Orr R, Nelson P, Barnes M, McLaughlin MJ, et al. 2019. The role of surface charge and ph changes in tropical soils on sorption behaviour of per- and polyfluoroalkyl substances (pfass). Science of The Total Environment 673:197-206.

Oliver DP, Li Y, Orr R, Nelson P, Barnes M, McLaughlin MJ, et al. 2020. Sorption behaviour of per- and polyfluoroalkyl substances (pfass) in tropical soils. Environmental Pollution 258:113726.

Paul AG, Jones KC, Sweetman AJ. 2009. A first global production, emission, and environmental inventory for perfluorooctane sulfonate. Environmental Science & Technology 43:386-392.

Pérez F, Nadal M, Navarro-Ortega A, Fàbrega F, Domingo JL, Barceló D, et al. 2013. Accumulation of perfluoroalkyl substances in human tissues. Environment International 59:354-362.

Persson J, Andersson N. 2016. Modeling groundwater flow and pfos transport. : A case study at the old fire drill site of bromma stockholm airport [Student thesis].

Phong Vo HN, Ngo HH, Guo W, Hong Nguyen TM, Li J, Liang H, et al. 2020. Poly-and perfluoroalkyl substances in water and wastewater: A comprehensive review from sources to remediation. Journal of Water Process Engineering 36:101393.

Prevedouros K, Cousins IT, Buck RC, Korzeniowski SH. 2006. Sources, fate and transport of perfluorocarboxylates. Environmental science & technology 40:32-44.

Puts GJ, Crouse P, Ameduri BM. 2019. Polytetrafluoroethylene: Synthesis and characterization of the original extreme polymer. Chemical Reviews 119:1763-1805.

Robey NM, da Silva BF, Annable MD, Townsend TG, Bowden JA. 2020. Concentrating per- and polyfluoroalkyl substances (pfas) in municipal solid waste landfill leachate using foam separation. Environmental Science & Technology 54:12550-12559.

Rodowa AE, Christie E, Sedlak J, Peaslee GF, Bogdan D, DiGuiseppi B, et al. 2020. Field sampling materials unlikely source of contamination for perfluoroalkyl and polyfluoroalkyl substances in field samples. Environmental Science & Technology Letters 7:156-163.

Saiers JE, Hornberger GM. 1996a. Modeling bacteria-facilitated transport of ddt. Water Resources Research 32:1455-1459.

Saiers JE, Hornberger GM. 1996b. The role of colloidal kaolinite in the transport of cesium through laboratory sand columns. Water Resources Research 32:33-41.

Saiers JE, Hornberger GM. 1999. The influence of ionic strength on the facilitated transport of cesium by kaolinite colloids. Water Resources Research 35:1713-1727.

Saiers JE. 2002. Laboratory observations and mathematical modeling of colloid-facilitated contaminant transport in chemically heterogeneous systems. Water Resources Research 38:1032.

Saiers JE, Lenhart JJ. 2003. Ionic-strength effects on colloid transport and interfacial reactions in partially saturated porous media. Water Resources Research 39:1256.

Schaefer CE, Culina V, Nguyen D, Field J. 2019. Uptake of poly- and perfluoroalkyl substances at the air–water interface. Environmental Science & Technology 53:12442-12448.

Schaefer CE, Nguyen D, Meng P, Fang Y, Knappe DRU. 2022. Sorption of perfluoroalkyl ether carboxylic acids (pfecas) at the air-water interface in porous media: Modeling perspectives. Journal of Hazardous Materials Advances 6:100062.

Schaider LA, Ackerman JM, Rudel RA. 2016. Septic systems as sources of organic wastewater compounds in domestic drinking water wells in a shallow sand and gravel aquifer. Science of The Total Environment 547:470-481.

Silva JAK, Martin WA, McCray JE. 2021. Air-water interfacial adsorption coefficients for pfas when present as a multi-component mixture. Journal of Contaminant Hydrology 236:103731.

Thompson JT, Chen B, Bowden JA, Townsend TG. 2023. Per- and polyfluoroalkyl substances in toilet paper and the impact on wastewater systems. Environmental Science & Technology Letters 10:234-239.

Thompson KA, Mortazavian S, Gonzalez DJ, Bott C, Hooper J, Schaefer CE, et al. 2022. Poly- and perfluoroalkyl substances in municipal wastewater treatment plants in the

united states: Seasonal patterns and meta-analysis of long-term trends and average concentrations. ACS ES&T Water 2:690-700.

U.S.EPA. 2021. Sw-846 test method 3512: Solvent dilution of non-potable waters. Available: https://www.epa.gov/hw-sw846/sw-846-test-method-3512-solvent-dilution-non-potable-waters.

USEPA. 2023. Per- and polyfluoroalkyl substances (pfas) proposed pfas national primary drinking water regulation.

USEPA. 2024. Cdr trend summary.

Vu CT, Wu T. 2022. Recent progress in adsorptive removal of per- and poly-fluoroalkyl substances (pfas) from water/wastewater. Crit Rev Env Sci Tec 52:90-129.

Wang J, Guo X. 2020. Adsorption isotherm models: Classification, physical meaning, application and solving method. Chemosphere 258:127279.

Wang J, Niven RK. 2021. Unification of surface tension isotherms of pfoa or genx salts in electrolyte solutions by mean ionic activity. Chemosphere 280:130715.

Wang W, Mi X, Zhou Z, Zhou S, Li C, Hu X, et al. 2019. Novel insights into the competitive adsorption behavior and mechanism of per- and polyfluoroalkyl substances on the anion-exchange resin. Journal of Colloid and Interface Science 557:655-663.

Wanzek T, Stults JF, Johnson MG, Field JA, Kleber M. 2023. Role of mineral–organic interactions in pfas retention by afff-impacted soil. Environmental Science & Technology 57:5231-5242.

WDNR, WDHS. 2019. Pfas contamination in marinette and peshtigo area.

Wei C, Song X, Wang Q, Hu Z. 2017. Sorption kinetics, isotherms and mechanisms of pfos on soils with different physicochemical properties. Ecotoxicology and Environmental Safety 142:40-50.

Yang Y, Saiers JE, Xu N, Minasian SG, Tyliszczak T, Kozimor SA, et al. 2012. Impact of natural organic matter on uranium transport through saturated geologic materials: From molecular to column scale. Environmental Science & Technology 46:5931-5938.

Zhao Y, Min X, Xu S, Wang Y. 2023. Adsorption of per- and polyfluoroalkyl substances (pfas) by aquifer materials: The important role of dolomite. Environmental Science & Technology Letters 10:931-936.

Zhou D, Brusseau ML, Zhang Y, Li S, Wei W, Sun H, et al. 2021. Simulating pfas adsorption kinetics, adsorption isotherms, and nonideal transport in saturated soil with tempered one-sided stable density (tosd) based models. Journal of Hazardous Materials 411:125169.